Supplementary Information

Table of content

		Static	PC	HPC	Native OA hACs
FRZB	Average	2,04E-02	5,04E-03	1,23E-03	6,03E-03
	Max	*2,10E-01*	*2,20E-02*	*8,60E-03*	*9,60E-03*
	Min	*1,60E-03*	*4,10E-04*	*1,20E-04*	*3,90E-03*
DKK1	Average	7,07E-04	6,15E-04	2,17E-04	2,70E-04
	Max	*4,20E-03*	*3,70E-03*	*1,00E-03*	*4,90E-04*
	Min	*3,50E-05*	*1,50E-05*	*8,10E-06*	*1,50E-04*
GREM1	Average	1,34E-02	1,08E-02	3,53E-03	7,00E-03
	Max	*3,60E-02*	*2,80E-02*	*1,40E-02*	*1,20E-02*
	Min	*1,40E-10*	*5,10E-10*	*1,10E-09*	*3,40E-03*

Table SI1. Selected genes expression (normalized to GAPDH) in static, PC and HPC CoC models (Donors = 5) and in native freshly isolated OA chondrocytes (Donors = 10).

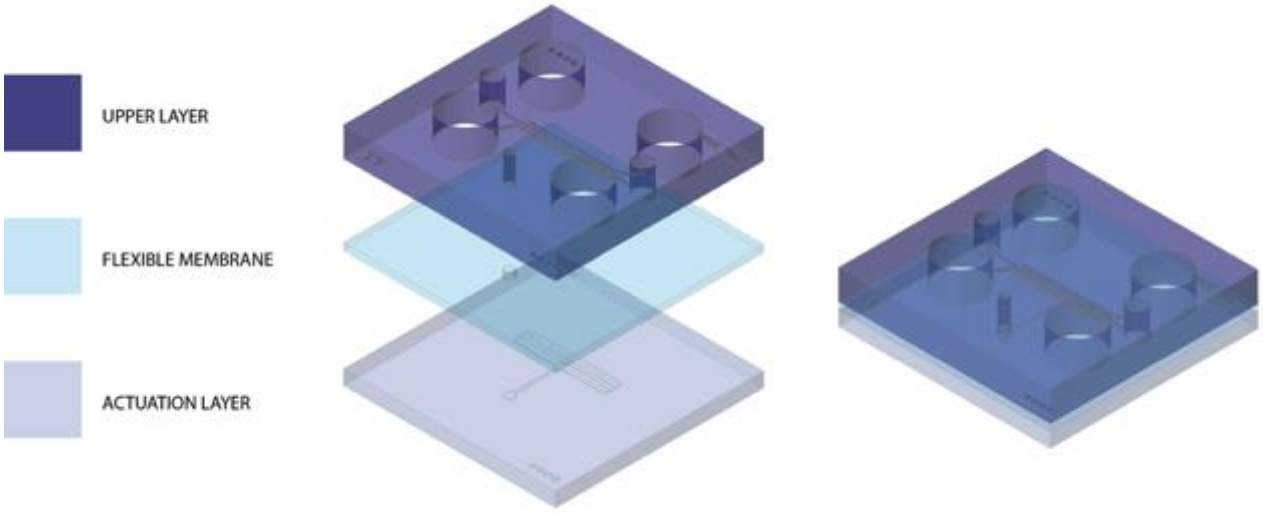

Figure SI1. Device production and assembly. PDMS layers were produced through replica molding and assembled through plasma bonding.

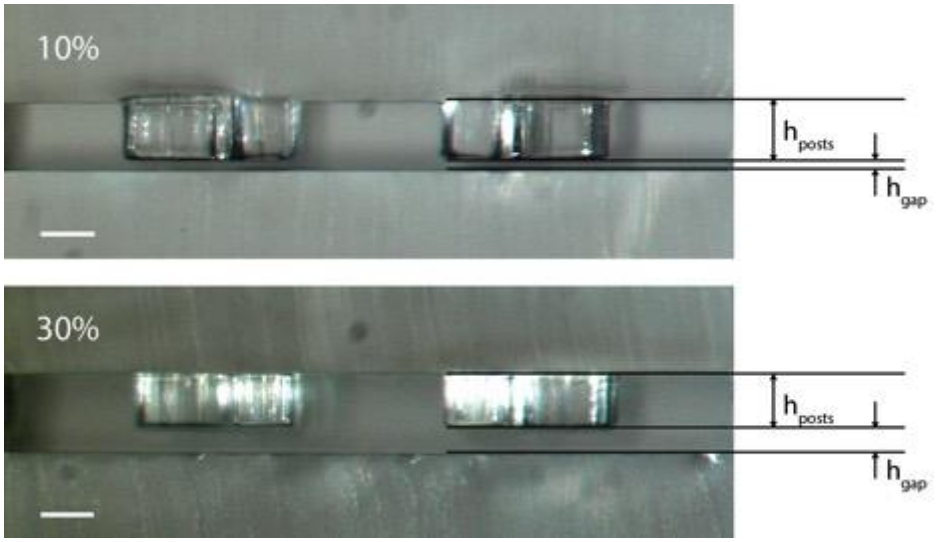

Fig. SI2 Gap and dimensions of the device. Stereomicroscope sections of the device. 10% and 30% versions are both presented. h_{posts} and h_{gap} indicates the heights of the hanging posts and of the gap respectively. Heights vary according to compression levels. 10%: h_{posts} = 129 μm, h_{gap} = 14 μm; 30% h_{posts}= 100 μm, h_{gap} = 43 μm. Scale bar 100 μm.

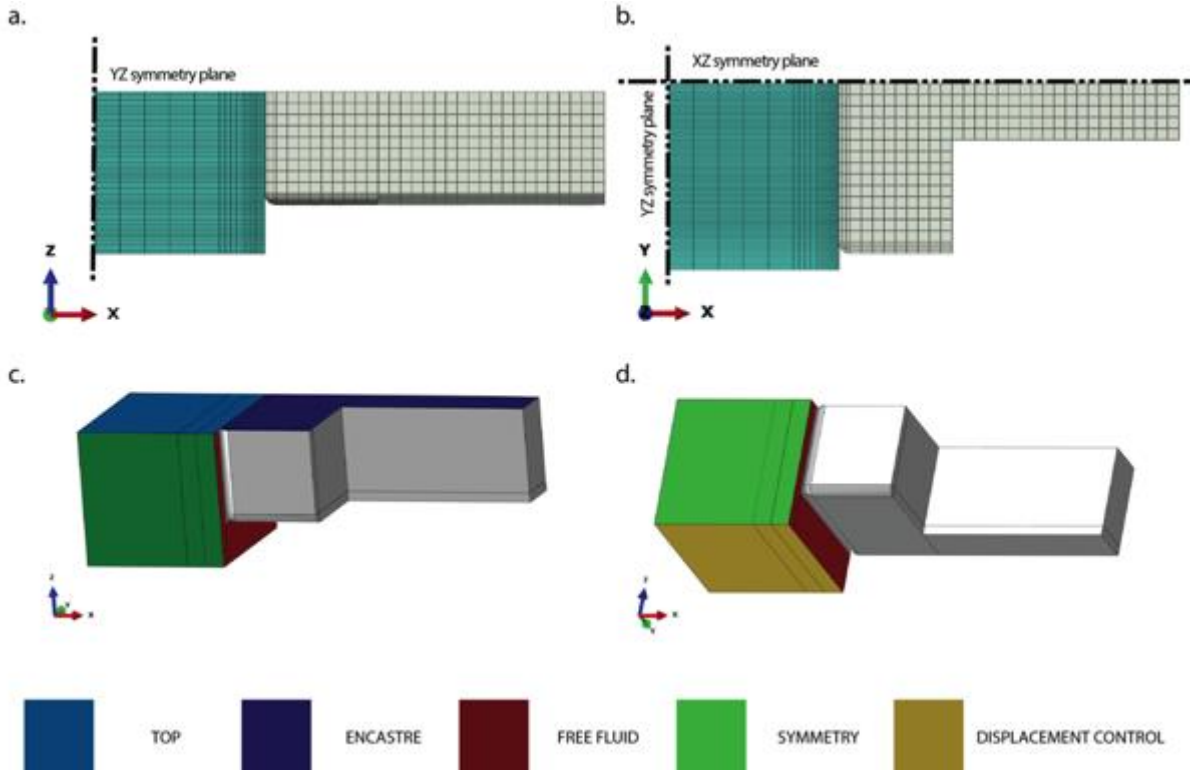

Fig. SI3 Numerical model boundary conditions. a. XZ lateral view. The YZ symmetry plane is highlighted. The adopted mesh is visible both in the construct (blue) and in the post (grey) **b. XY** top view. The XZ and YZ symmetry planes are highlighted. The adopted mesh is visible both in the hydrogel (blue) and in the post (grey). **c.** 3D model schematization, top view. **d.** 3D model schematization. Bottom view. Boundary conditions are indicated with a color code. Cyan: top; Blue: encastre; Red: free fluid; Green: symmetry; Yellow: displacement control.

Actuation pressure characterization and flexible membrane thickness optimization

The compression value applied to the construct depends on the flexible PDMS membrane stroke, that is to say from the gap between flexible membrane and posts bottom surface. To reach abutment of the membrane against the hanging posts bottom face an adequate pressure has to be applied to the actuation chamber. This pressure depends on the membrane material properties, on its geometry and on the resistance to compression of the CoC. Notably the CoC properties evolve in time as the constructs becomes more mature. To avoid dependence of the applied compressive strain to the construct mechanical resistance, the PDMS flexible membrane thickness was tailored to make the CoC resistance to compression negligible with respect to the membrane flexional rigidity. This way, the exactly wanted compressive stroke can be applied, once provided the adequate pressure. The following experiment was carried out to determine the optimal membrane thickness and the required actuation pressure. A blue dye was injected in the culture medium channels with the central gel channel filled either with PEG gel or again with blue dye. Given the optical transparency of PDMS, in resting position the hanging posts appeared, therefore, blue given the fluid meatus present between their lower surface and the membrane below (Fig SI4a, b). Upon gradual increase of the pressure in the actuation chamber, the height of the meatus decreases and the color of the posts lightens up, until it reaches a plateau when the membrane abuts against the pillars (Fig SI4c, d). The color intensity in an area within posts cross section was measured through an image J built in function and plotted against the applied pressure (Fig. SI4e). The actuation pressure was defined as the onset of the plateau. The described experiment was repeated increasing gradually the thickness of the membrane. The minimal thickness that allowed for the actuation pressure obtained with and without the gel to be equals was adopted (i.e. 750 μm). The optimization process was referred to the most demanding between the two compression levels under investigation, namely the 30%.

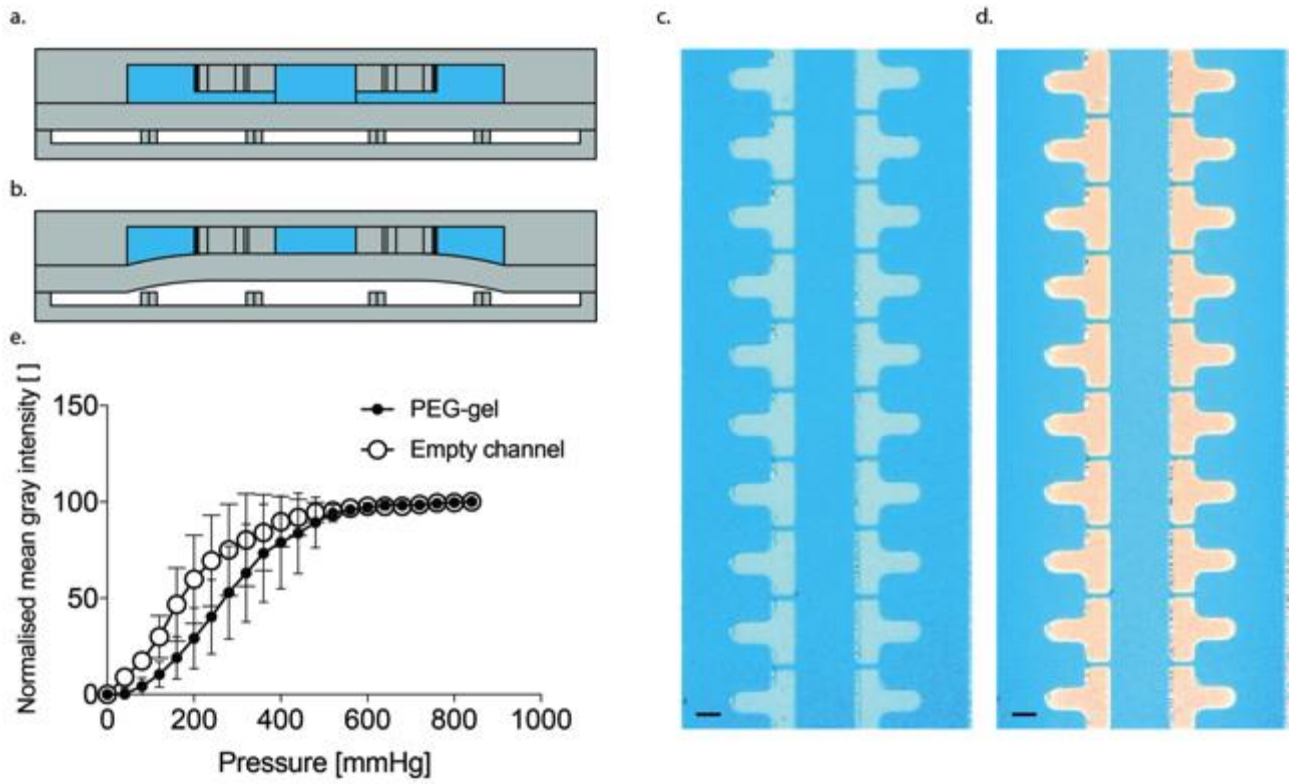

Fig. SI4 Characterization of actuation pressure. a, Device schematization, rest state. **b,** Device schematization, compressed state. **c,** Brightfield image of the top chamber. Rest state (relative pressure, p=0 mmHg). Both central channel and medium channels were filled with blue dye. Posts appear blue given the dye filled gap between posts end and actuation membrane. Reference background was subtracted to enhance picture luminosity. Scale bar 100 μm. **d,** Brightfield image of the top chamber. Compressed state (relative pressure p = 600 mmHg). Both central channel and medium channels were filled with blue dye. Under pressure the membrane is in contact with posts bottom surface. Posts appear therefore white. Reference background was subtracted to enhance picture luminosity. Scale bar 100 μm. **e,** Normalized mean gray intensity versus pressure in the actuation chamber measured in areas within the posts cross section. Experiments were performed leaving the central channel empty or filling it with the adopted PEG gel formulation. Chips with a 750 μm membrane were adopted; n = 6 devices were considered for each condition. Measurements were performed in n = 3 different areas for each device and averaged. Results are expressed as mean ± SD. Background mean gray intensity obtained at atmospheric pressure was subtracted from subsequent measurements. Results are expressed as percentage of the mean gray intensity obtained at the highest pressure applied (840 mmHg) to normalize for lighting conditions. Results refer to 30% compression devices, the most critical in terms of actuation pressure. Complete adherence of the actuation membrane to the bottom surface of the posts is evidenced by mean gray intensity plateau onset. Plateau onset pressure (p ~= 500 mmHg) does not vary with or without the gel presence given a sufficient actuation membrane thickness.

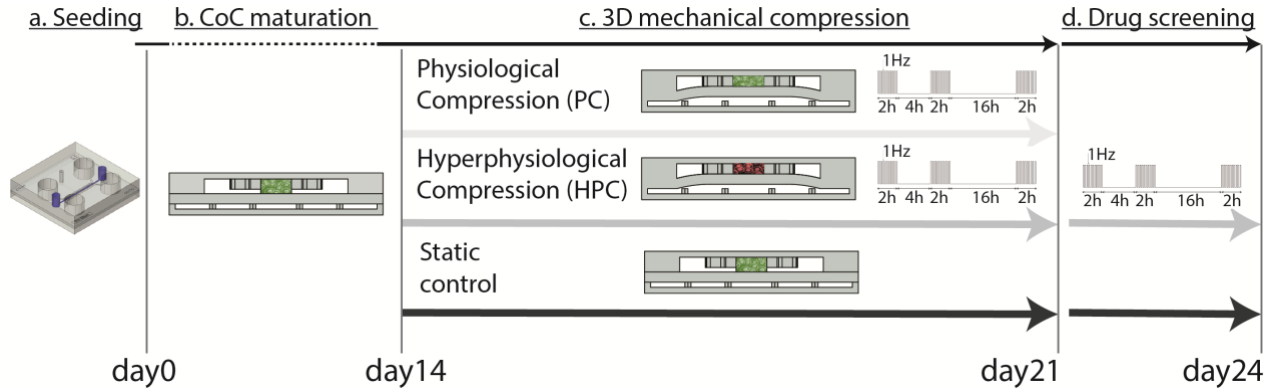

Fig. SI5 Experimental plan. a, Human articular chondrocytes (hACs) isolated from healthy donors were embedded in PEG gel and injected into the microscale platform. **b,** 14 days of chondrogenic culture under static condition leads to the generation of a CoC. **c,** Two different levels of mechanical compression were then applied for seven additional days, physiological (i.e. PC, 10%) and hyper-physiological (i.e. HPC, 30%). A static condition was included as control. **d,** While maintaining a HPC, anti-inflammatory/anti-degrading compounds were supplemented to the model and their effect analysed after three additional days.

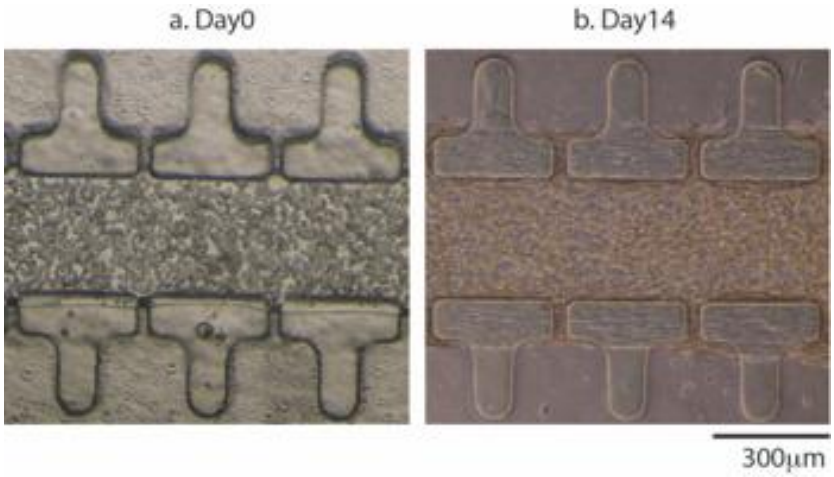

Fig. SI6 Phase contrast images of day0 and day14 to show the distribution of cells at the beginning and the confinement of matrix along the culture: this clarify that we control geometry and we finally apply the load as we computationally estimated. Experiments were repeated with n ≥ 45 biologically independent samples from 5 different donors with similar results.

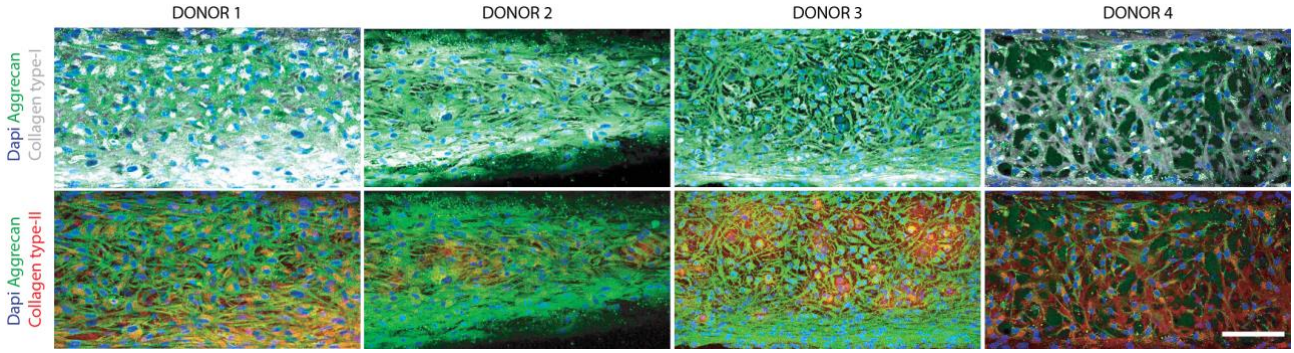

Fig SI7 Cartilage like matrix deposition after 14 days of static culture. Scale bar 100μm. 15 biologically independent samples from 5 different donors were considered. An image per donor is reported**.**

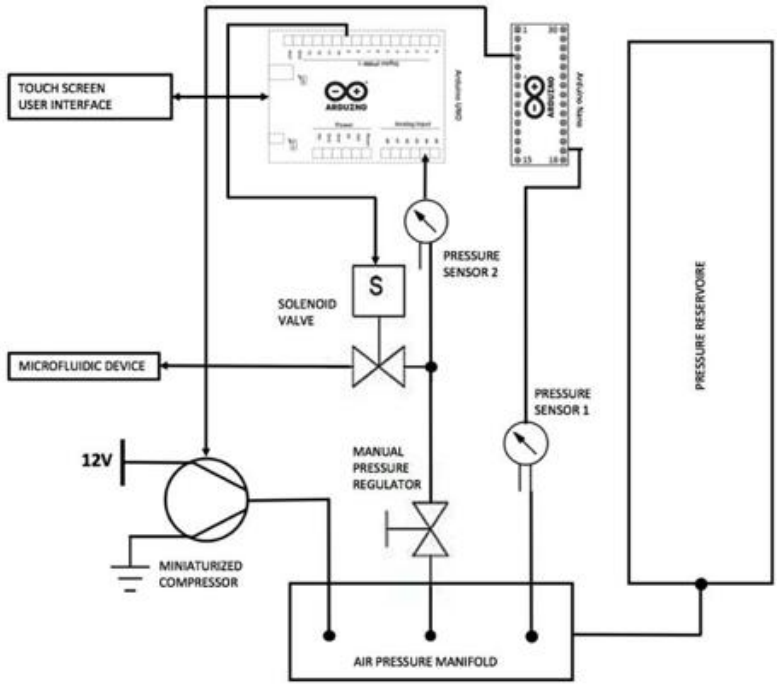

Fig. SI8 Electro-pneumatical actuation system. Single components and connections are schematized.

Cell viability

Cell viability was assessed in both stimulated CoC tissues after 14 days of maturation in static culture and 7 days of mechanical stimulation, by performing a LIVE/DEAD Assay (Life Technologies) according to the manufacturer's protocol. Briefly, after washing with PBS, devices were perfused with a 2 µM calcein AM and 4 µM Ethidium homodimer-1 solution and subsequently incubated for 30 mins at 37°C. Confocal images of labeled cells were acquired with a fluorescence Nikon A1R Nala Confocal microscope (Nikon, Tokyo, Japan), green-labeled cells and red-stained nuclei representing live and dead cells, respectively (Fig. SI9).

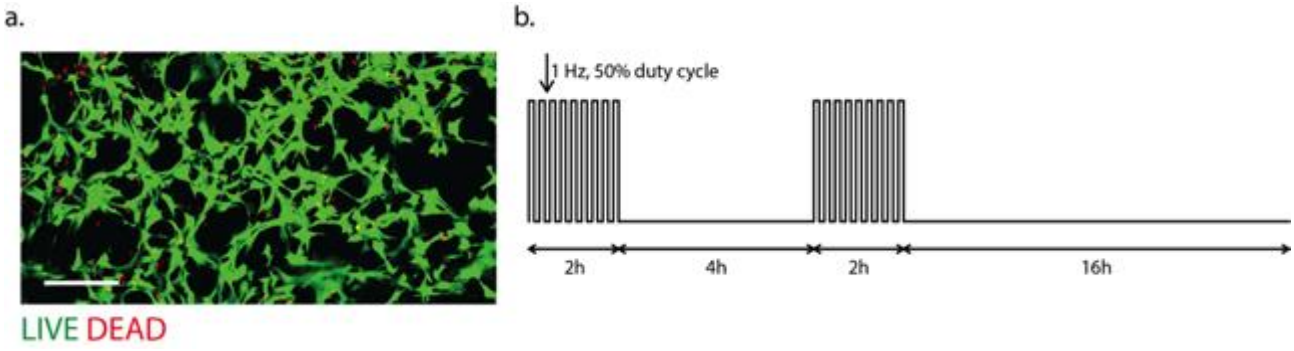

Fig. SI9 Live/Dead. a, LIVE/DEAD assay of CoC. A 30% compression was applied, for 7 consecutive days with the pattern presented in **b,** following 14 days of static culture in chondrogenic differentiation medium. Scale bar 100 µm. (n=3 biologically independent samples were considered from a single donor). **b,** Applied stimulation pattern. Each day two 2 hours cycles were divided by a 4 hours pause. Cyclical compression was provided with a frequency of 1Hz and applying the actuation pressure with a 50% duty cycle.

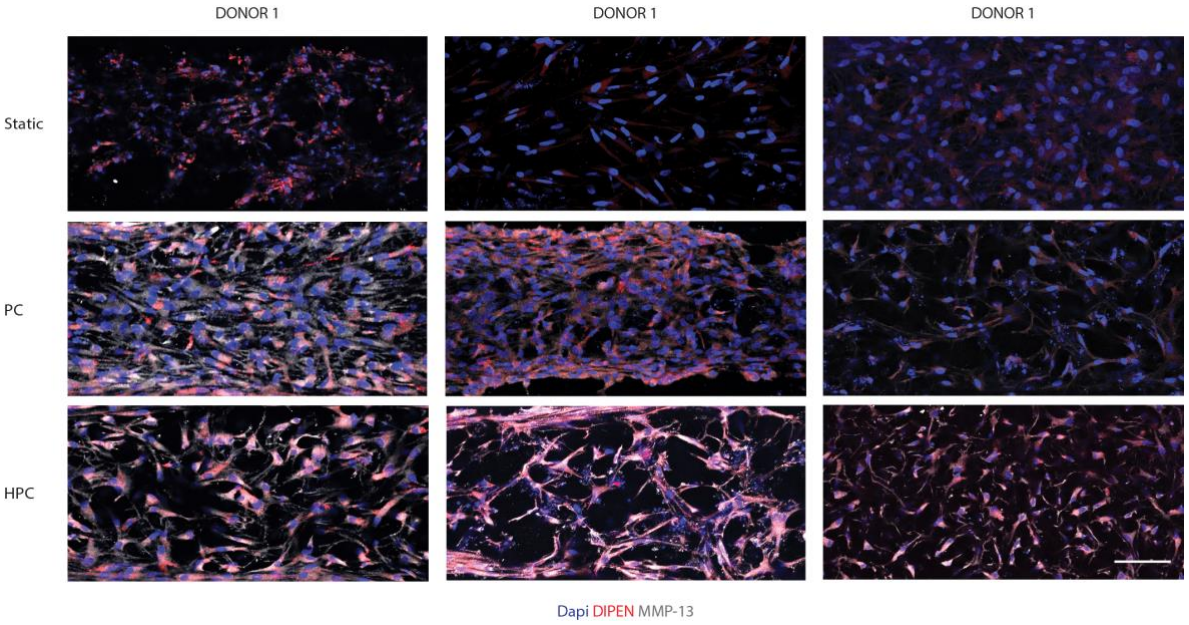

Fig. SI10 MMP13 and DIPEN expression upon PC and HPC stimulation. Scale bar 100µm. 9 biologically independent samples from 3 different donors were considered. An image per donor is reported**.**

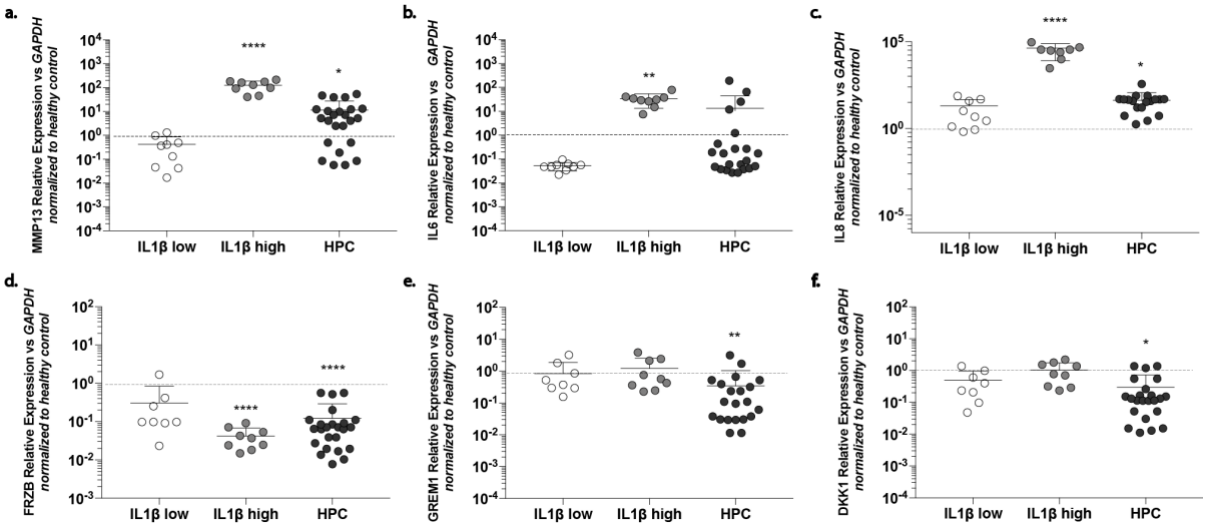

Fig. SI11 Comparison between traditional "cytokine-based" models and HPC-based CoC in modulating degradation, inflammation and hypertrophy brakes. a, Expression of genes responsible for cartilage degradation (*MMP13*), **b, c,** inflammation (*IL6* and *IL8*) and **d, e, f,** cartilage hypertrophy brakes (*FRZB, DKK1*, and *GREM1*) was measured by RT-PCR (n=21 biologically independent samples from 5 different donors were considered for 3D HPC and healthy control; n=9 biologically independent samples from 3 different donors were considered for IL1β high, 2D 3D IL1β low and 3D IL1β high). Results are mean + SD. Statistics by statistics by Kruskal-Wallis test with Dunn's multiple comparison test for non-normal distributions in all graphs where statistical analysis is reported. **a,** *P = 0.0304; **b,** **P = 0.0025; **c,** *P = 0.0113; **e,** **P = 0.0082; **f,** *P = 0.0129. ****P < 0.0001 in all graphs. The HPC stimulus was compared to "cytokine-based" treatments with high (1ng/ml) and low (10pg/ml) doses of IL1β. All gene expression values are normalized relative to GAPDH expression and refer to basal expression in the corresponding healthy control; values are log scale. Statistical significance was calculated against the respective healthy control.

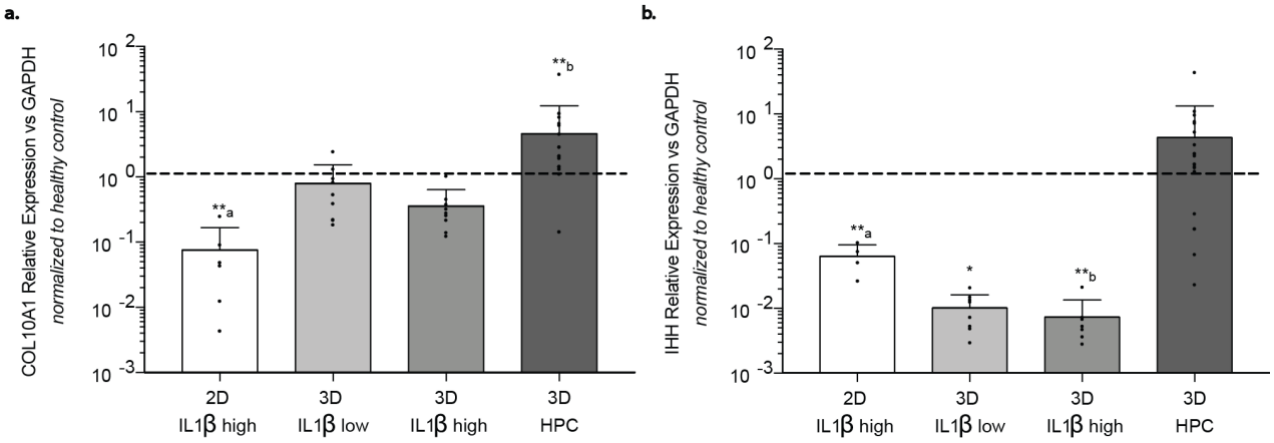

Fig. SI12 Comparison between traditional "cytokine-based" models (both in 2D or inside the 3D CoC model), and HPC-based CoC in modulating chondrocytes hypertrophy. a, b, Expression of genes responsible for cartilage hypertrophic differentiation (*COL10A1, IHH*) was measured by RT-PCR (n=24 biologically independent samples from 5 different donors were considered for 3D HPC and controls; n=6 biologically independent samples from 3 different donors were considered for 3D IL1β low and 3D IL1β high, n=6 biologically independent samples from 2 different donors were considered for 2D IL1β high and 2D control). Treating a chondrocytes monolayer with a high dose of IL1β resulted in a significant reduction of *COL10A1* and *IHH* expression as compared to the 2D healthy control. Both the same treatment or a lower dose

applied to the 3D CoC model didn't lead to any change in *COL10A1* and *IHH* expression as compared to the 3D healthy control. The application of a HPC to the 3D CoC model upregulated *COL10A1* and *IHH* gene expression, as compared to the 3D healthy control, coherently with the induction of an OA-like phenotype. All gene expression values are normalized relative to GAPDH expression and refer to basal expression in the corresponding healthy control; values are log scale. Statistical significance was calculated against the respective healthy control. Results are mean + SD. Statistics by two tailed Mann-Whitney for 2D culture and by Kruskal-Wallis test with Dunn's multiple comparison test for non-normal distributions for 3D culture in all graphs where statistical analysis is reported. **a,** **aP = 0.0022 **bP = 0.0014; **b,** *P = 0.0201, **aP = 0.0095, **bP = 0.0073. Individual experimental data era represented by the black dots overlaid to histograms.

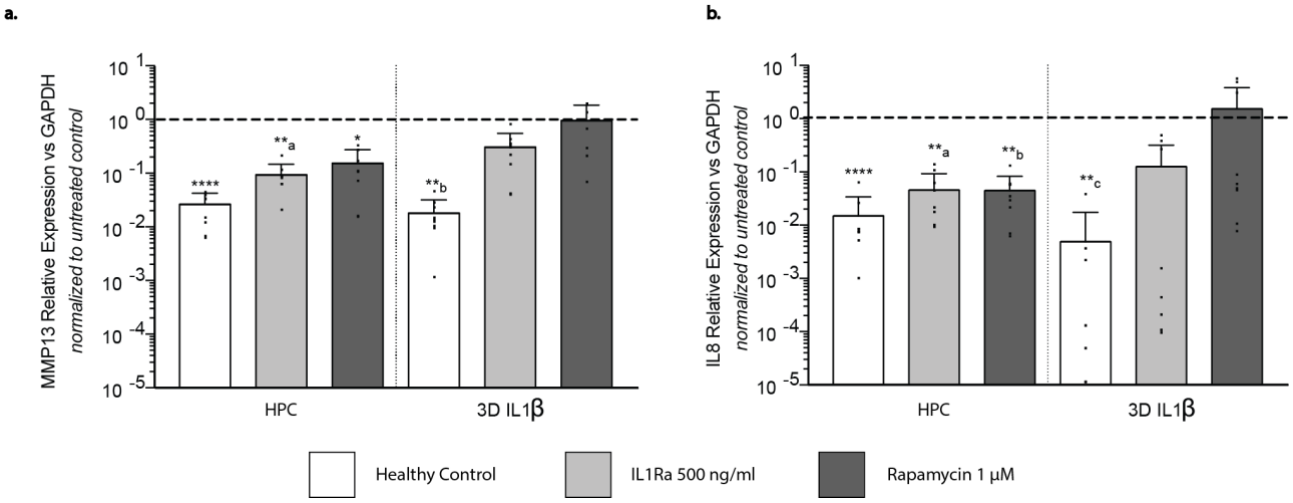

Fig. SI13 Drug screening: comparison between the proposed HPC model and a 3D "Cytokine-based" model, both established within the CoC. a, b, The expression of *MMP13* and *IL8* in response to subministration of two known anti-inflammatory/anti-degrading compounds (i.e. Il1Ra and Rapamycin) was evaluated by RT-qPCR both on HPC and "cytokine-based" (i.e. 1ng/ml IL1β) models. DMSO was used as vehicle. All gene expression values are normalized relative to GAPDH expression and refer to the basal expression in the untreated (i.e. HPC CoC supplemented with DMSO only) control; values are log scale. The mean expression value of the untreated control (i.e. HPC CoC supplemented with DMSO only) is represented by the black horizontal line. PCR (n=9 biologically independent samples from 3 different donors were considered). Statistical significance was calculated against the respective untreated control. Results are mean + SD, *. Statistics by one-way ANOVA and Bonferroni's multiple comparison test or Dunnett's multiple comparison tests (normal distributions), or Kruskal-Wallis test with Dunn's multiple comparison test (non-normal distributions) in all graphs where statistical analysis is reported. **a,** *P = 0.0322, **aP = 0.0076, **bP = 0.0042; **b,** **aP = 0.0043 , **bP = 0.0050, **cP = 0.0070; ****P < 0.0001. Individual experimental data era represented by the black dots overlaid to histograms.

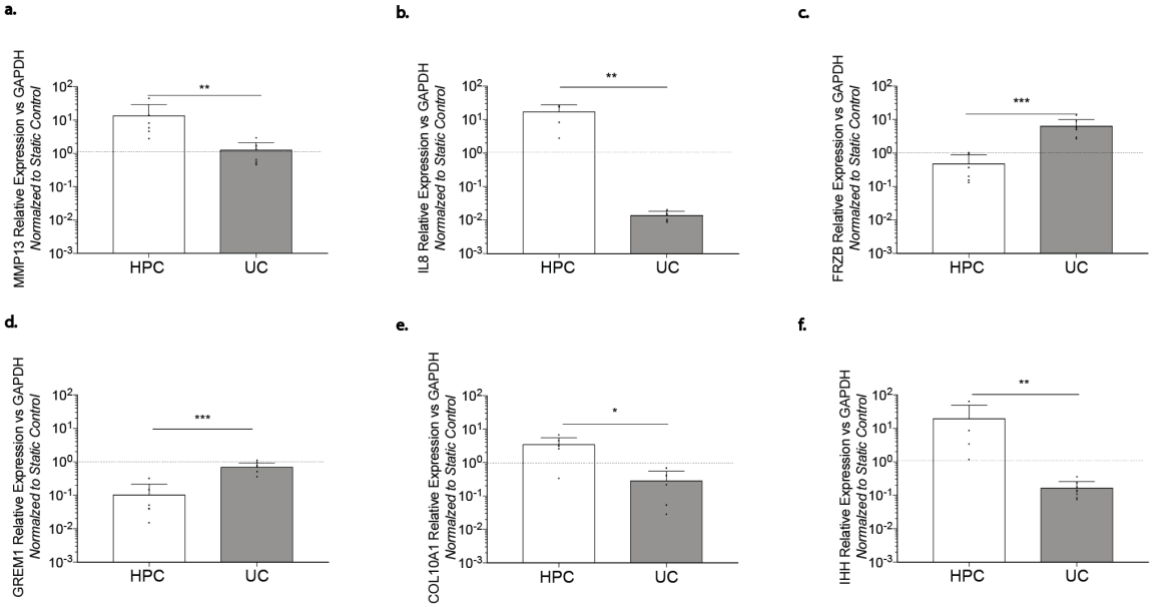

Fig SI14 Comparison between Hyper Physiological confined compression (HPC) and Hyperphysiological Unconfined Compression (UC). a, Expression of genes responsible for cartilage degradation (*MMP13*), **b,** inflammation (*IL8*) **c, d,** cartilage hypertrophy brakes (*FRZB,* and *GREM1*), and **e, f.** hypertrophy was measured by RT-PCR (n=9 biologically independent samples from 3 different donors were considered). The HPC stimulus was compared to an Unconfined compression (UC) stimulus of the same magnitude (i.e. 30%) using a previously reported microfluidic device, with similar dimensions and construction but where the microconstructs are able to expand laterally upon compression[1]. All gene expression values are normalized relative to GAPDH expression and refer to basal expression in the corresponding static control; values are log scale. Statistical significance was calculated comparing HPC and UC. Static controls expression level is indicated by the horizontal dotted line. Results are mean + SD, Statistics by Two tailed Mann-Whitney test (non-normal distributions). **a,** **P = 0.0013; **b,** **P = 0.0016; **c,d** ***P < 0.001; **e,** *P = 0.0173; **f,** **P = 0.0040. Individual experimental data era represented by the black dots overlaid to histograms.

Movie S1. PEG hydrogel strain field upon 30% compression. Nominal strains in the ii direction NE_{ii} are reported. (NE_{xx} left, NE_{yy} top right and NE_{zz} bottom right). Min and max values are reported throughout the compression.

Movie S2. 3D reconstruction of the CoC in static culture (left) of after HPC (right). Dapi (blue), MMP-13 (grey) and DIPEN (red) expression were analysed by immunofluorescence staining. Reconstruction do not span the entire CoC thickness. Reconstructions highlight an increased MMP13 expression and colocalisation of DIPEN and MMP13 upon 30% compression.

References

1. Marsano, A. *et al.* Beating heart on a chip: a novel microfluidic platform to generate functional 3D cardiac microtissues. *Lab Chip* **16,** 599–610 (2016).